Journal of Solid State Chemistry 182 (2009) 2762–2768

Contents lists available at ScienceDirect

Journal of Solid State Chemistry

journal homepage: www.elsevier.com/locate/jssc

# Correlation between optical constants and crystal chemical parameters of $ZrW_2O_8$

Robert D. Shannon [a], Reinhard X. Fischer [b,*], Olaf Medenbach [c], Eric Bousquet [d], Philippe Ghosez [d]

[a] Geological Sciences/CIRES, University of Colorado, Boulder, CO 80309, USA
[b] Universität Bremen, FB 5 Geowissenschaften, Klagenfurter Straße, D-28359 Bremen, Germany
[c] Institut für Mineralogie, Fakultät für Geowissenschaften, Ruhr-Universität Bochum, Universitätsstraße 150, D-44780 Bochum, Germany
[d] Département de Physique, Université de Liège, B-5, B-4000 Sart Tilman, Belgium

ARTICLE INFO

*Article history:*
Received 3 February 2009
Received in revised form
4 July 2009
Accepted 18 July 2009
Available online 25 July 2009

*Keywords:*
$ZrW_2O_8$
Refractive indices
Optical dispersion
Electronic polarizability
Born effective charges

ABSTRACT

The refractive indices of $ZrW_2O_8$, measured at wavelengths of 435.8–643.8 nm, were used to calculate $n_D$ at $\lambda = 589.3$ nm and $n_\infty$ at $\lambda = \infty$ from a one-term Sellmeier equation. Refractive indices, $n_D$ and dispersion values, $A$, are, respectively, 1.8794 and $114 \times 10^{-16}$ m$^2$. The high dispersion, relative to other molybdates, tungstates and Zr-containing compounds, is attributed to the low value of $E_o = 7.7$ eV and mean cation coordination number. Total electronic polarizabilities, $\alpha_{total}$, were calculated from $n_\infty$ and the Lorenz–Lorentz equation. The unusually large difference between the observed polarizability of 20.087 Å$^3$ and the calculated total polarizability $\alpha_T$ of 17.59 Å$^3$ ($\Delta = +12.4\%$) is attributed to (1) a large $M$–O–W angle, (2) a high degree of W $5d$–$O_{(terminal)}$ $2p$ and Zr $nd$–O $2p$ hybridization, and (3) unusually high oxygen displacement factors, $B$(O), normalized to $B$(W).



## 1. Introduction

$ZrW_2O_8$ is unusual because of its negative thermal expansion coefficient over the range 0.3–1050 K [1]. The refractive index, $n_D$, of $ZrW_2O_8$ was reported to be 1.669 [1], but this value appears to be rather low for a tungstate. Other tungstates such as $CaWO_4$, $SrWO_4$, $BaWO_4$, $ZnWO_4$ and $PbWO_4$ have $n_D$ values ranging from 1.84 to 2.27. In this paper we report the redetermination of the refractive index and the optical dispersion of $ZrW_2O_8$ with an emphasis on its total polarizability and the correlation between its crystal chemical parameters ($M$–O–$M'$ angles of bridging O atoms with metal ions, equivalent isotropic oxygen displacement factors, and Born effective charges ($Z^*$) of metal and oxygen atoms). Here we attempt to explain the unusually large deviation of the experimentally redetermined value of total electronic polarizability from the calculated polarizability by (1) comparison of $M$–O–$M'$ angles in $ZrW_2O_8$ with $M$–O–$M'$ angles in other compounds having bridging oxygen atoms, (2) analysis of oxygen displacement factors in $ZrW_2O_8$ and (3) calculation of Born effective charges of Zr, W, and O.

## 2. Experimental and computational details

The sample used for refractive index measurements was a clear, colorless fragment about $3 \times 2 \times 1.5$ mm$^3$ in size. An analysis of the crystal using a CAMECA CAMEBAX SX-50 electron-microprobe, wavelength-dispersive spectrometers, and the PAP matrix correction procedure [2] resulted in the composition $Zr_{1.019}W_{1.988}O_8$. The principal method of preparation of small crystal prisms and the procedure for measuring the refractive index and dispersion were described in detail by Medenbach and Shannon [3] together with a comprehensive discussion of the errors involved in the minimum-deviation method. The error limits are estimated to be less than $\Delta n = \pm 0.0005$.

First-principles calculations have been performed using the density functional theory (DFT) formalism and a pseudopotential/plane-wave approach as implemented in the ABINIT package [4]. We used Teter pseudopotentials [5], considering as valence electrons the $2s$ and $2p$ levels of O atoms, the $4s$, $4p$, $4d$ and $5s$ levels of Zr atoms and the $5s$, $5p$, $5d$ and $6s$ levels of W atoms. The local density approximation (LDA) was used to approximate the exchange–correlation energy while a cut-off energy of 45 Ha on the plane-wave expansion and a $2 \times 2 \times 2$ Monkorsh-Pack mesh of $k$-points gave converged results on the quantities of interest (violation of the Born effective charge neutrality less than $0.01e$). The Born effective charges and the electronic dielectric tensor were determined by linear response using density functional perturbation theory [6].

* Corresponding author.
*E-mail address:* rfischer@uni-bremen.de (R.X. Fischer).

0022-4596/$ - see front matter © 2009 Elsevier Inc. All rights reserved.
doi:10.1016/j.jssc.2009.07.035

**Table 1**
Experimental and calculated (LDA) non-equivalent atomic positions (reduced coordinates) (with Wyckoff site symbols in parentheses) for $ZrW_2O_8$ in the cubic structure with the space group No.198 ($P2_13$).

| | Experimental [1] | LDA (present study) |
|---|---|---|
| Zr (4*a*), $x=y=z$ | 0.0004 | 0.0030 |
| W1 (4*a*), $x=y=z$ | 0.3409 | 0.3428 |
| W2 (4*a*), $x=y=z$ | 0.6009 | 0.5964 |
| O1 (4*a*), $x=y=z$ | 0.4941 | 0.4876 |
| O2 (4*a*), $x=y=z$ | 0.2322 | 0.2359 |
| O3 (12*b*) | | |
| *x* | 0.0529 | 0.0577 |
| *y* | −0.2069 | −0.2038 |
| *z* | −0.0619 | −0.0606 |
| O4 (12*b*) | | |
| *x* | 0.0697 | 0.0644 |
| *y* | −0.0575 | −0.0520 |
| *z* | 0.2132 | 0.2184 |

**Table 2**
Experimental refractive indices, optical dispersion values *A*, *B* [Eq. (1)], single oscillator values $E_d$, $E_o$ [Eq. (4)], and total polarizabilities $\alpha_T$ [Eq. (2)] of $ZrW_2O_8$.

| wavelength $\lambda$ (nm) | *n* |
|---|---|
| 643.8 | 1.8709 |
| 576.9 | 1.8819 |
| 546.0 | 1.8887 |
| 508.6 | 1.8984 |
| 480.0 | 1.9087 |
| 468.0 | 1.9139 |
| 435.8 | 1.9294 |
| *A* | $114\times10^{-16}$ m$^2$ |
| *B* | 0.4279 |
| $E_o$ | 7.73 eV |
| $E_d$ | 18.07 eV |
| $n_\infty$ ($\lambda=\infty$) | 1.8268 |
| $n_D$ ($\lambda=589.3$ nm) | 1.8794 |
| $\alpha_T$ | 20.087 Å$^3$ |

The calculations were performed at the experimental volume, with a cell parameter $a=9.1546$ Å, and the atomic positions were relaxed until the residual force on any atom is less than $10^{-5}$ Ha/Bohr. The experimental and calculated atomic positions are compared in Table 1. The theoretical accuracy is satisfactory and comparable to that previously achieved in LDA calculations on comparable systems [7]. Our LDA calculation predicts for the relaxed structure an indirect electronic bandgap of 3.8 eV (between *R* and *X* points), which surprisingly overestimates a previously reported theoretical value of 2.84 eV [8]. As discussed below, our calculation nevertheless provides a refractive index $n_\infty$ in good agreement with the experiment. Moreover, reducing the bandgap to its experimental estimate using a scissor correction [9] makes the agreement significantly worse, which leads us to suggest the real amplitude of the bandgap in α-$ZrW_2O_8$ may be higher than 2.8 eV.

## 3. Results

Table 2 lists refractive indices of $ZrW_2O_8$ as a function of $\lambda$ and the dispersion parameters *A*, *B*, $E_o$ and $E_d$ obtained by fitting to the one-term Sellmeier expression used by Wemple and Domenico [10]:

$$\frac{1}{n^2-1}=-\frac{A}{\lambda^2}+B \tag{1}$$

where *A*, the slope of the plot of $(n^2-1)^{-1}$ vs. $\lambda^{-2}$, gives a measure of the dispersion and *B*, the intercept of the plot at $\lambda=\infty$ gives $n_\infty=(1+1/B)^{1/2}$. Calculated values of $n_\infty$ and $n_D$ were derived from the dispersion plots. The calculated value of the total electronic polarizability, 20.087 Å$^3$, was determined from the Lorenz–Lorentz equation:

$$\alpha_T=\frac{1}{b}V_m\cdot\frac{n_\infty^2-1}{n_\infty^2+2} \tag{2}$$

where the Lorentz factor *b* is defined as $b=4\pi/3$, $V_m$ the molar volume in Å$^3$, and $n_\infty$ the refractive index at $\lambda=\infty$. The observed value of $n_D$ was found to be 1.8794, significantly higher than the value of 1.669 reported in [1]. We also note that the reported value $n_\infty=1.8268$ in Table 2 is in qualitative agreement with our first-principles LDA result of $n_\infty=1.90$. Using a scissor correction that adjusts the calculated bandgap to its estimated experimental value we get however a still larger value $n_\infty=1.95$, suggesting that the real bandgap could be larger than expected and, a priori, still larger than our theoretical value.

## 4. Discussion

### 4.1. Deviation of total experimental from calculated polarizability of $ZrW_2O_8$

In Shannon and Fischer [11], total electronic polarizabilities were calculated from a set of empirical polarizabilities in conjunction with a polarizability additivity rule to give agreement to within 4% with 387 experimental total polarizabilities of oxides, hydroxides, oxyhydroxides, oxyfluorides, oxychlorides, and hydrates. Using these polarizabilities [11] and

$$\alpha_T(ZrW_2O_8)=\alpha_e(Zr^{4+})+2\alpha_e(W^{6+})+8\alpha_e(O^{2-}) \tag{3}$$

where $\alpha_e(Zr^{4+})=2.023$ Å$^3$, $\alpha_e(W^{6+})=2.500$ Å$^3$, and $\alpha_e(O^{2-})=1.321$ Å$^3$, we calculate the total electronic polarizability $\alpha_T$ of $ZrW_2O_8$ to be 17.59 Å$^3$. Thus the observed value, 20.087 Å$^3$, shows a large discrepancy, ($\Delta=\alpha_{obs}-\alpha_{calc}$), of +12.4% from the calculated polarizability. In the above study [11], $\Delta$ values greater than +4% were found in crystal structures with corner-shared octahedra characterized by network and chain structures involving infinite Ti–O–Ti, Nb–O–Nb, or Ta–O–Ta chains such as the $AMO_3$ perovskites $CaTiO_3$, $SrTiO_3$, $BaTiO_3$, $KNbO_3$, and $KTaO_3$ and tungsten–bronze type compounds such as $Ba_{1-x}Sr_xNb_2O_6$. In addition, two compounds, $Tb_2Mo_3O_{12}$ and $Gd_2Mo_3O_{12}$, with *hetero-ion* Tb–O–Mo and Gd–O–Mo networks formed mostly from corner-shared Tb(Gd)$O_7$ and $MoO_4$ groups showed moderately large $\Delta=4.0\%$ and 3.4% values [11]. $ZrW_2O_8$, having a structure characterized primarily by corner-shared $ZrO_6$ and $WO_4$ groups, is yet another example of a compound with *hetero-ion* chains, Zr–O–W, that shows large deviations of observed from calculated total electronic polarizability.

To better understand the $ZrW_2O_8$ structure, we compare it with $Tb_2Mo_3O_{12}$ and $Gd_2Mo_3O_{12}$. Fig. 1 shows that the $ZrW_2O_8$ bridging oxygen O1 and O2 are shared between $ZrO_6$ and $WO_4$ groups (W–O distances = 1.79 and 1.81 Å), O3 is "quasi-terminally" bonded to W2 at 1.72 Å and O4 is terminally bonded to W1 at 1.71 Å [1]. "Quasi-terminal" O3 is different from O4 in that the W2–O3 distance is slightly longer than the W1–O4 distance (1.71 Å) because of weak interaction of O3 with W1 at 2.41 Å [1]. The Zr–O–W bonds in $ZrW_2O_8$ are similar in nature to the Tb(Gd)–O–Mo bonds but differ in detail in that the ⟨Zr–O–W⟩ angles are larger (163°) than the ⟨Tb(Gd)–O–Mo⟩ bonds (156°) with *d*(Mo–O) = 1.70–1.83 Å and there are terminal oxygen atoms in $ZrW_2O_8$. In addition, only $\frac{5}{6}$ of the O's in

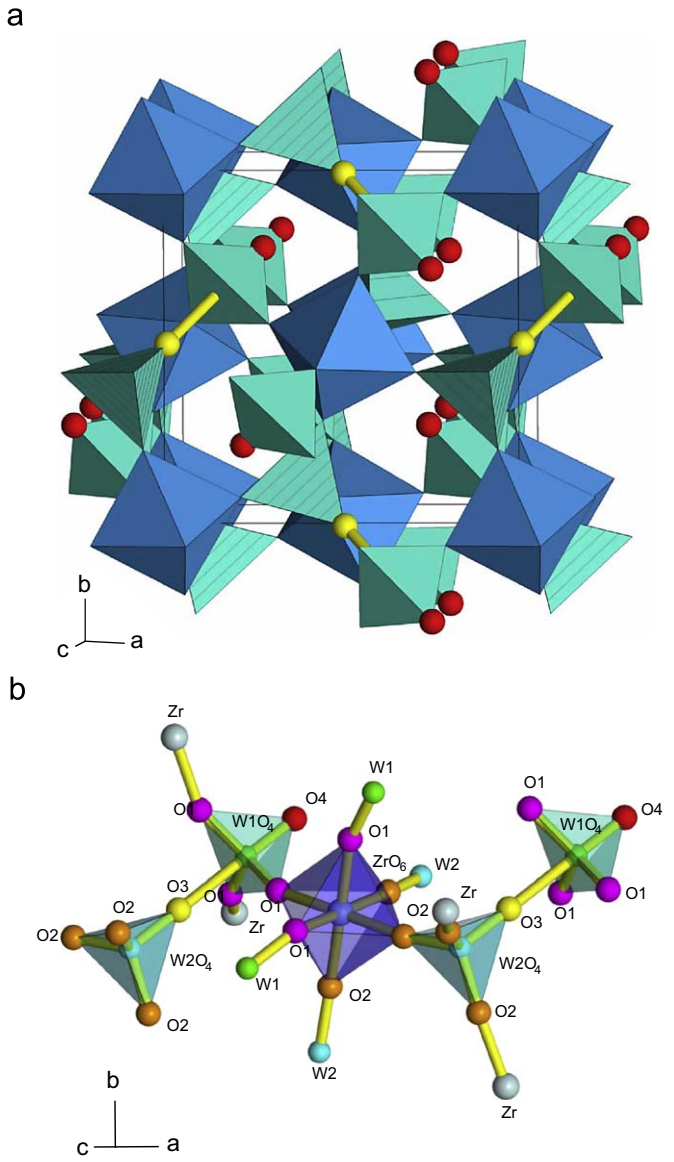


**Fig. 1.** Projections of the crystal structure of $ZrW_2O_8$ after [12]: (a) projection parallel **c** rotated by 3° about **a** and **b**. $WO_4$ tetrahedra are green ($W1O_4$ plane, $W_2O_4$ hatched), $ZrO_6$ octahedra are blue. Terminal O4 atoms are shown as red spheres, pseudoterminal O3 atoms are yellow with long bonds to W1 and (b) projection of the local environments of the cations and anions parallel **c** rotated by 20° about **b**. (For interpretation of the references to the color in this figure legend, the reader is referred to the web version of this article.)

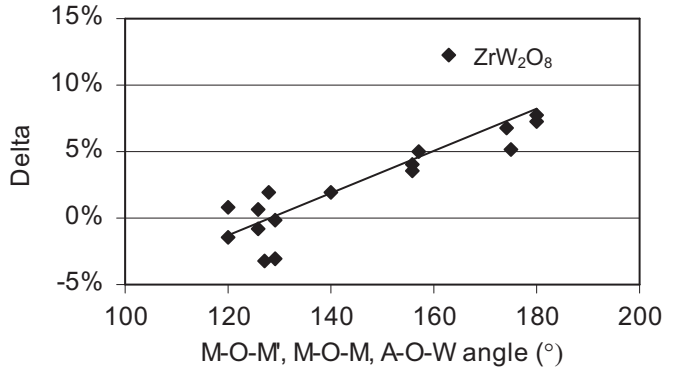


**Fig. 2.** Delta vs. ⟨*M*–O–*M*′⟩, ⟨*M*–O–*M*⟩, and ⟨*A*–O–W⟩ angles for titanates, niobates, tantalates, molybdates, and tungstates. The solid line represents the linear regression omitting $ZrW_2O_8$.

**Table 3**
Deviations of observed from calculated total polarizability vs. ⟨*M*–O–*M*⟩, ⟨*M*–O–*M*′⟩ or ⟨*A*–O–W⟩ angle.

| Compound[a] | Number of data points | ⟨*M*–O–*M*⟩, ⟨*M*–O–*M*′⟩, and ⟨*A*–O–W⟩ angles[a] | Deviation[a] $\Delta$ (%) |
|---|---|---|---|
| Titanates | | | |
| $TiO_2$ (rutile) | 2 | 120 | −1.4 |
| $TiO_2$ (anatase) | 3 | 120 | 0.8 |
| $CaTiO_3$ | 1 | 157 | **5.0** |
| $SrTiO_3$ | 6 | 180 | **7.8** |
| $BaTiO_3$ | 2 | 175 | **5.1** |
| Niobates and tantalates | | | |
| $LiNbO_3$ | 3 | 140 | 1.9 |
| $KNbO_3$ | 3 | 174 | **6.8** |
| $KTaO_3$ | 1 | 180 | **7.3** |
| Molybdates and tungstates | | | |
| $Nd_2Mo_3O_{12}$ | 1 | 126 | −0.6 |
| $Tb_2Mo_3O_{12}$ | 1 | 148 | **4.0** |
| $Gd_2Mo_3O_{12}$ | 2 | 148 | **3.4** |
| $ZnWO_4$ | 3 | 128 | 2.0 |
| $CaWO_4$ | 3 | 126 | −0.8 |
| $SrWO_4$ | 1 | 127 | −3.2 |
| $BaWO_4$ | 1 | 129 | −3.1 |
| $PbWO_4$ | 4 | 129 | −0.1 |
| $Sc_2W_3O_{12}$ | 1 | 157 | – |
| $Y_2W_3O_{12}$ | 1 | 160 | – |
| $ZrW_2O_8$ | 1 | 163 | **12.4** |

[a] Data from [11]; bold numbers indicate unusually high values of $\Delta$ where ($\Delta = \alpha_{obs} - \alpha_{calc}$).

$Tb(Gd)_2Mo_3O_{12}$ are purely bridging bonds; $\frac{1}{6}$ are bonded to 1 Mo and 2 Tb(Gd) with Tb(Gd)–O–M angles of 126°.

#### 4.1.1. *Effect of M–O–M′ angle*

Enhanced polarizabilities in compounds containing Ti–O–Ti, Nb–O–Nb, or Ta–O–Ta chains were attributed to increased covalence of the *M*–O–*M* (O bridging two metal ions *M* of the same kind) bonds associated with anomalously large Born effective charges (BEC's) of both *M* and O atoms and increased *M*–O–*M* angles. The interdependence of $\Delta$, ⟨*M*–O–*M*⟩ angle (angle brackets indicate mean values) and BEC's in the titanates, niobates and tantalates was attributed [11] to the degree of covalence determined by orbital overlap of oxygen 2*p* states with metal *d* states increasing as the *M*–O–*M* angle approaches 180°. Because BEC's had not been calculated for $Tb_2Mo_3O_{12}$ and $Gd_2Mo_3O_{12}$, we first looked for a correlation of $\Delta$ with *M*–O–*M* angle(s) in perovskites, *M*–O–*M*′ angle(s) in $Tb_2Mo_3O_{12}$, $Gd_2Mo_3O_{12}$, and $ZrW_2O_8$ and *A*–O–W angle(s) in $AWO_4$ compounds (O bridging different metal ions) associated with titanate, niobate, tantalate, molybdate and tungstate structures. Fig. 2 shows a composite diagram of ⟨*M*–O–*M*⟩, ⟨*M*–O–*M*′⟩ and ⟨*A*–O–W⟩ angles in titanates, niobates, tantalates, molybdates and tungstates. Although the data are limited we see in Table 3 and Fig. 2 a good correlation between $\Delta$ values and angles but with $ZrW_2O_8$ well above the line formed from the titanates, niobates, tantalates, molybdates and other tungstates. We conclude that Zr–O–W angles alone cannot explain the unusually large $\Delta$ value and that $ZrW_2O_8$ must have characteristics, not present in other tungstates and molybdates, that contribute to the unusually large $\Delta$ value of $ZrW_2O_8$.

#### 4.1.2. *Contribution of oxygen displacement factors*

Next, we explore the possible contribution of oxygen displacement factors to the large $\Delta$ value of $ZrW_2O_8$. In [11], equivalent isotropic displacement factors of oxygen, *B*(O), normalized to

**Table 4**
Oxygen displacement factors in $ZrW_2O_8$.

| Compound | $\langle B(O)\rangle$ (Å$^2$) | $\langle B(W)\rangle$ (Å$^2$) | $\langle B(O)\rangle/B(W)\rangle$ | $\Delta$ (%) | Method[a] | $R$ (%) | Reference |
|---|---|---|---|---|---|---|---|
| $CaWO_4$ | $B(O) = 0.772$ | 0.459 | 1.68 | −0.8 | XRD-S | 2.3 | [13] |
| $CaWO_4$ | $B(O) = 0.777$ | 0.410 | 1.89 | −0.8 | XRD-S | 3.2 | [14] |
| $ZrW_2O_8$ | | | | | | | |
| O(bridging) | $\langle B(O)\rangle = 2.28$ | | | **12.4** | ND-P | 6.5 | [15] |
| O(terminal) | $\langle B(O)\rangle = 3.45$ | | | | | | |
| $ZrW_2O_8$ | | | | | | | |
| O(bridging) | $\langle B(O)\rangle = 1.69$ | 0.80 | 1.93 | **12.4** | ND-P | 2.4 | [16] |
| O(terminal) | $\langle B(O)\rangle = 2.94$ | 0.80 | 3.36 | | | | |
| $ZrW_2O_8$ | | | | | | | |
| O(bridging) | $\langle B(O)\rangle = 1.56$ | 0.63 | 2.48 | **12.4** | ND-P | 3.1 | [1] |
| O(terminal) | $\langle B(O)\rangle = 2.78$ | 0.63 | 4.41 | | | | |
| $ZrW_2O_8$ | | | | | | | |
| O(bridging) | $\langle B(O)\rangle = 1.307$ | 0.478 | 2.73 | **12.4** | ND-P | 9.6 | [12] |
| O(terminal) | $\langle B(O)\rangle = 2.29$ | 0.478 | 4.79 | | | | |
| Average of bridging O's | | | $\langle$**2.35**$\rangle$ | | | | |
| Average of terminal O's | | | $\langle$**4.19**$\rangle$ | | | | |
| Mean of br and term O's | | | $\langle$2.81$\rangle$ | | | | |

[a] XRD: X-ray diffraction, ND: neutron diffraction, S: single crystal, P: powder.

$B(M)$, were considered as a factor to help explain the high $\Delta$'s of compounds containing Ti–O–Ti, Nb–O–Nb, or Ta–O–Ta chains. However, this connection was not pursued in detail because of the better correlation of $\Delta$ with $M$–O–$M$ angle. In the case of $ZrW_2O_8$ the "bridging" oxygen atoms, O1 and O2, and quasi-terminal O3 have high equivalent isotropic displacement factors $B(O)$, of 1.59, 1.35 and 1.75 Å$^2$, [average = 1.56 Å$^2$] respectively, and normalized to $B(W)$, $\langle B(O)/B(W)\rangle = 2.48$, and $B(O)$ of terminal O4 has the exceptionally high value of 2.78 Å$^2$ [$(B(O)/B(W) = 4.41$] [1]. In Table 4 we summarize oxygen displacement factors in $ZrW_2O_8$ and compare them to $\langle B(O)\rangle$ and $\langle B(O)\rangle/\langle B(W)\rangle$ of 0.78 and 1.78 Å$^2$, respectively, in $CaWO_4$ [13,14] where O has 1 W and 2 Ca near neighbors and no Ca–O–W chains. The displacement factors of the bridging oxygen atoms of $ZrW_2O_8$ deviate in the same sense as in Fig. 2 with larger values of $\Delta$ whereas the terminal oxygen of $ZrW_2O_8$ has significantly larger values of $B(O)/B(W)$. Thus, we conclude that bridging oxygen thermal parameters are important determinants of $\Delta$ but that the terminal oxygen atoms in $ZrW_2O_8$ may have a dominant influence on $\Delta$, i.e., oxygen polarizability, $\alpha(O_{terminal})$, is higher than the normal polarizability of non-terminal oxygen atoms, $\alpha(O_{non\text{-}terminal})$.

### 4.1.3. *Born effective charges in $ZrW_2O_8$*

The Born effective charges tensor $Z^*_{\kappa,\alpha\beta}$ of an atom $\kappa$ is related to the change of the spontaneous polarization $P_\alpha$ produced by the displacement of the sublattice of atom $\kappa$ in direction $\beta$ under the condition of zero macroscopic electric field $E$:

$$Z^*_{\kappa,\alpha\beta} = \Omega \frac{\partial P_\alpha}{\partial \tau_{\kappa,\alpha}}|_{(E=0)}$$

where $\alpha$ and $\beta$ label the Cartesian coordinates [17]. According to this definition, high values of the BEC's can lead to large polarization, even for small displacements. This was used as the fingerprint of the ferroelectric instability in the family of $ABO_3$ perovskite compounds like $BaTiO_3$, where the BEC of Ti and O along the Ti–O direction are anomalously large: +7.2$e$ for Ti and −5.8$e$ for O instead of a nominal ionic charge of +4$e$ and −2$e$, respectively [17]. These anomalous BEC's were related to dynamical charge transfers occurring along the Ti–O chain when the bond length is modified, which is related to hybridization changes between the O 2$p$ and the Ti 3$d$ orbitals [17,18]. Furthermore,

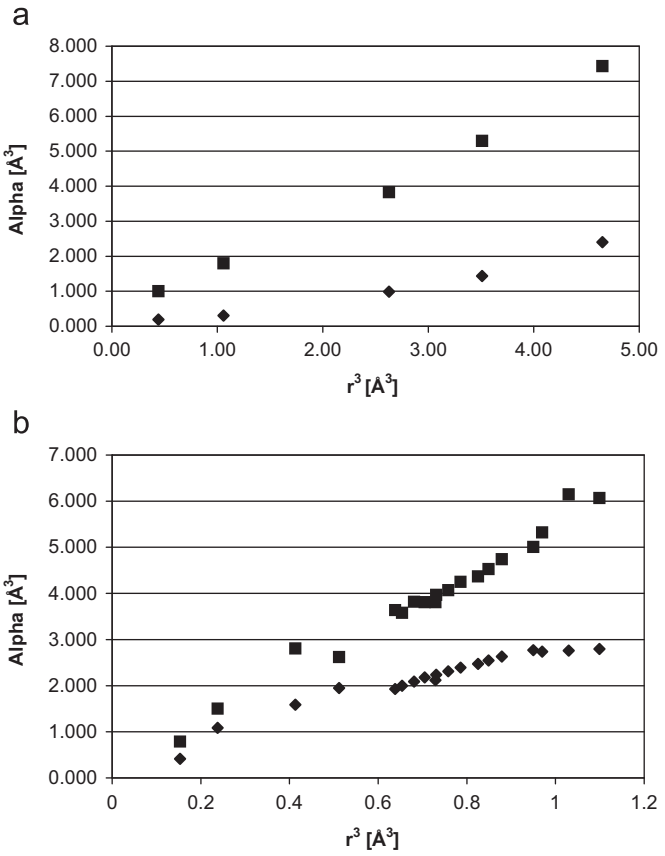


**Fig. 3.** Dielectric (squares) and electronic (diamond symbols ) polarizabilities of monovalent and trivalent cations vs. $r^3$: (a) polarizability of $M^+$ vs. $r^3$ and (b) polarizability of $M^{3+}$ vs. $r^3$.

these anomalous BEC's have been associated with high electronic polarizability [17,19,20]. They involve both ionic and electronic polarizabilities, the sum of which have been termed "dielectric polarizabilities" derived from dielectric constants in the KHz–MHz range [21]. Because the set of dielectric polarizabilities in [21] did not take cation coordination into consideration, we cannot strictly correlate them with BEC values. However, because

of the strong correlation between dielectric and electronic polarizabilities (see Figs. 3a and b), we assume that the trends in $\Delta$ values derived from dielectric polarizabilities approximate the trends in $\Delta$ values derived from electronic polarizabilities.

Although we have shown correlations of $\Delta$ with $M$–O–W angles and oxygen displacement factors, we should be able to get a more fundamental understanding of the origin of the discrepancy between observed and calculated polarizabilities by looking at Born effective charges (BEC's), which reflect dynamical charge transfers and hybridization changes between oxygen $p$ and metal $d$ states. Charge transfer resulting from hybridization between Ti 3$d$ and O 2$p$ states in $BaTiO_3$ was demonstrated by Cohen and Krakauer [22] using "first-principles" calculations where they found static charges lower than nominal charges and corresponding to $Ba^{2+}Ti^{2.89+}O_3^{1.63-}$. The BEC's calculated from first principles might be a complementary tool to describe charge transfer [17,18].

To get more insight into the unusually high $\Delta$ values of $ZrW_2O_8$, the Born effective charge tensors have been calculated and are listed in Table 5. The oxygen BEC's are all highly anisotropic: the bridging oxygen atoms, O1 and O2, similar to the bridging oxygen atoms in the titanate ($A^{2+}TiO_3$) and niobate ($A^{+}NbO_3$) perovskites show strong $Z^*(O)$ anisotropy with $Z^*(O)_{\parallel} \gg Z^*(O)_{\perp}$ where the $O_{\parallel}$ and $O_{\perp}$ terms refer to oxygen displacements parallel and perpendicular to the $M^{n+}$–$O^{2-}$–$M'^{n+}$ chain, respectively. In Table 5, we also report the eigenvalues of the symmetric part of the Born effective charge tensors of $ZrW_2O_8$ (present study) along with the previously published data for $Y_2W_3O_{12}$ [7] and $WO_3$ [23]. Although all reported BEC values for Zr are anomalously high with values ranging from 4.63$e$ to 6.03$e$ [24,25] (see the summary for BEC's of cubic $ZrO_2$, tetragonal $ZrO_2$, monoclinic $ZrO_2$, $ZrSiO_4$, $BaZrO_3$ and $PbZrO_3$ in [11]), the values of $Z^*$(Zr) in $ZrW_2O_8$ are even higher (+7.45$e$ and +6.68$e$, compared to the nominal ionic charge of +4$e$). In contrast, however, $Z^*$(W) in $ZrW_2O_8$ (between +3.63$e$ and +5.36$e$) is quite different and considerably smaller than its value in the defect perovskite $WO_3$ (+12.5$e$). $Z^*$(W) is in fact surprisingly small in comparison to the nominal charge of +6$e$. The values of $Z^*$(W) are of the same order of magnitude in $Y_2W_3O_{12}$ (between +3.09$e$ and +4.21$e$). The differences in $Z^*$(W) in $ZrW_2O_8$ vs. $Z^*$(W) in $WO_3$ can probably be ascribed to the coordination of $W^{6+}$, resulting in lower $Z^*$(W) for tetrahedral $W^{6+}$ in $ZrW_2O_8$ and $Y_2W_3O_{12}$ than $Z^*$(W) with octahedral $W^{6+}$ in $WO_3$. Similar BEC differences were noted for quartz [26] and stishovite [27] where $Z^*$ (tetrahedral $Si^{4+}$) = between 3.02$e$ and 3.45$e$ compared to $Z^*$ (octahedral $Si^{4+}$) = between 3.80$e$ and 4.05$e$. Further confirmation of this hypothesis must await the calculation of BEC's in other compounds containing tetrahedral $W^{6+}$ such as $CaWO_4$ and octahedral $W^{6+}$ insert space such as $ZnWO_4$. The cause of the unusually low $Z^*$(W) in $ZrW_2O_8$ could arise from different W 5$d$–O 2$p$ hybridization in $WO_3$ and $ZrW_2O_8$, resulting from tetrahedral $WO_4^{2-}$ groups in $ZrW_2O_8$ and octahedral $WO_6^{6-}$ groups in $WO_3$. Sumithra et al. [7] have suggested that the low $Z^*$(W) in $Y_2W_3O_{12}$ may be associated with the reverse ordering of the $e_g$ and $t_{2g}$ orbitals in tetrahedral $W^{6+}$ coordination.

The BEC's of O1 and O2 in ZrW2O8 ($Z^*(O1)_{\parallel} = 3.72e$ and $Z^*(O2)_{\parallel} = 2.19e$) are smaller than the BEC's of the bridging oxygen atoms in the ferroelectric titanates ($A^{2+}TiO_3$) and niobates ($A^{+}NbO_3$), [mean = 5.7$e$ (range = 3.8$e$–7.1$e$)], but the effective charge of the terminal oxygen atoms, $Z^*(O3)_{\parallel} = -4.65e$ and $Z^*(O4)_{\parallel} = -5.26e$, is of the same order of magnitude than the perovskite oxygen atoms (see Table VIII in [11] for a tabulation of $Z^*_O$ in Ti, Zr, Nb and Ta perovskites). This suggests that the presence of terminal oxygen

**Table 5**
Calculated Born effective charge tensors ($e$) for inequivalent atoms of $ZrW_2O_8$ (present study).

| | $ZrW_2O_8$ | $Y_2W_3O_{12}$ | $WO_3$ |
|---|---|---|---|
| Zr | $\begin{pmatrix} 7.19 & -0.06 & -0.45 \\ -0.45 & 7.19 & -0.06 \\ -0.06 & -0.45 & 7.19 \end{pmatrix}$ [7.45; 7.45; 6.68] | Y [5.25; 4.85; 4.53] | |
| $W_1$ | $\begin{pmatrix} 5.23 & -0.13 & -0.13 \\ -0.13 & 5.23 & -0.13 \\ -0.13 & -0.13 & 5.23 \end{pmatrix}$ [5.36; 5.36; 4.97] | W [4.06; 4.04; 3.09] | W [12.51,12.51,12.51] |
| $W_2$ | $\begin{pmatrix} 4.42 & -0.35 & -0.44 \\ -0.44 & 4.42 & -0.35 \\ -0.35 & -0.44 & 4.42 \end{pmatrix}$ [4.82; 4.82; 3.63] | W [4.21; 3.88; 3.34] | |
| $O_1$ | $\begin{pmatrix} -1.62 & -1.06 & -1.04 \\ -1.04 & -1.62 & -1.06 \\ -1.06 & -1.04 & -1.62 \end{pmatrix}$ [−3.72; −0.57; −0.57] | O [−4.08; −0.69; −0.58] | O [−9.13; −1.68; −1.68] |
| $O_2$ | $\begin{pmatrix} -1.24 & -0.49 & -0.46 \\ -0.46 & -1.24 & -0.49 \\ -0.49 & -0.46 & -1.24 \end{pmatrix}$ [−2.19; −0.77; −0.77] | O [−4.18; −0.66; −0.59] | |
| $O_3$ | $\begin{pmatrix} -1.58 & 1.48 & 0.94 \\ 1.53 & -4.25 & 0.94 \\ 0.96 & -1.52 & -1.57 \end{pmatrix}$ [−4.65; −2.11; −0.64] | O [−4.37; −0.65; −0.61] | |
| $O_4$ | $\begin{pmatrix} -0.92 & 1.39 & -0.93 \\ 0.14 & -0.92 & 1.00 \\ -0.93 & 0.97 & -4.75 \end{pmatrix}$ [−5.26; −0.15; −1.17] | O [−3.66; −0.68; −0.67] | |
| | | O [−3.68; −0.67; −0.63]<br>O [−3.83; −0.77; −0.60] | |

The eigenvalues ($e$) of the symmetric part of the tensors are also given in bracket for $ZrW_2O_8$ (present study), $Y_2W_3O_{12}$ [7] and $WO_3$ [23].

**Table 6**
Refractive indices and optical dispersion of zirconium, molybdenum and tungsten-containing oxides[a].

| Compound | $\langle n_D \rangle$[a] | Dispersion ($10^{16}$ m$^2$) | $E_o$ (eV obs[a]) | $\langle N_c \rangle$ | $E_d$ (eV obs[a,b]) | $E_d$ (eV[b] calculated) | $\Delta$ ($E_d$) | $\Delta$ (%) |
|---|---|---|---|---|---|---|---|---|
| $ZnWO_4$ | 2.237 | 82 | 7.3 | 6.0 | 26.50 | 25 | 1.5 | 2.0 |
| $CaWO_4$ | 1.925 | 73 | 9.2 | 6.0 | 23.60 | 25 | 1.4 | −0.8 |
| $SrWO_4$ | 1.865 | 74 | 9.6 | 6.0 | 22.60 | 25 | 2.4 | −3.2 |
| $BaWO_4$ | 1.842 | 76 | 9.6 | 6.0 | 21.90 | 25 | 3.1 | −3.1 |
| $PbWO_4$ | 2.246 | 104 | 6.6 | 6.0 | 23.50 | 25 | 1.5 | −0.1 |
| | Mean | ⟨82⟩ | ⟨8.5⟩ | | | | | |
| $Zr_{.894}Y_{.095}Hf_{.011}O_{1.95}$ | 2.170 | 58 | 8.9 | 7.8 | 31.10 | 32 | 0.9 | 0.5 |
| $Zr_{.869}Y_{.131}O_{1.934}$ | 2.158 | 59 | 8.9 | 7.7 | 30.60 | 31.9 | 1.3 | 0.0 |
| $Zr_{.671}Y_{.329}O_{1.835}$ | 2.069 | 72 | 8.5 | 7.3 | 26.10 | 30 | 3.9 | −1.4 |
| $ZrSiO_4$ | 1.943 | 64 | 9.7 | 6.0 | 25.70 | 25 | 0.7 | 3.7 |
| $ZrSiO_4$ | 1.945 | 57 | 10.3 | 6.0 | 27.40 | 25 | 2.4 | 4.6 |
| $Zr_{.99}Hf_{.01}SiO_4$ | 1.945 | 58 | 10.2 | 6.0 | 27.00 | 25 | 2 | 3.9 |
| $ZrSiO_4$ | 1.954 | 54 | 10.5 | 6.0 | 23.40 | 25 | 1.6 | 4.4 |
| $Tb_2Mo_3O_{12}$ | 1.871 | 103 | 8.2 | 5.2 | 19.00 | 21.6 | 2.6 | 4.0 |
| $Gd_2Mo_3O_{12}$ | 1.862 | 101 | 8.3 | 5.2 | 19.00 | 21.6 | 2.6 | 3.3 |
| **$ZrW_2O_8$** | 1.8794 | **114** | **7.73** | **4.7** | 18.07 | 19.4 | 1.3 | 12.4 |

[a] Data from [28].
[b] $E_d = \beta \times Z_a \times N_e \times \langle N_c \rangle$; $\beta = 0.26$ eV; $Z_a = 2$; $N_e = 8$; and $\langle N_c \rangle$ = mean cation CN.

atoms in $ZrW_2O_8$ contributes significantly to the large value of $\Delta$ in Fig. 2.

*In summary*: the large $\Delta$ of $ZrW_2O_8$ relative to that of other tungstates and $Tb(Gd)_2Mo_3O_{12}$ is likely caused by (1) the large Zr–O–W angles and (2) the presence of terminal O4 and "quasi-terminal" O3 with (a) their large oxygen displacement values and (b) probably large hybridization of W 5*d*–$O_{(terminal)}$ 2*p* and Zr *nd*–O 2*p* orbitals.

### 4.2. Dispersion of $ZrW_2O_8$

In Shannon et al. [28], the range of dispersions from 50 to $80 \times 10^{-16}$ m$^2$ was designated "normal dispersion", and $80-250 \times 10^{-16}$ m$^2$ "high dispersion". In Table 6 we note the relatively high dispersion of $114 \times 10^{-16}$ m$^2$ of $ZrW_2O_8$. High dispersion was associated with the presence of $s^2$ ions such as $As^{3+}$, $Sb^{3+}$, $Tl^{+}$, and $Pb^{2+}$ but not associated with the presence of Zr or W. This is confirmed in Table 6 by comparing dispersion of $ZrW_2O_8$ with the Zr oxides, $Zr_{1-x}Y_xO_{2-x/2}$ and $ZrSiO_4$ having $A = 54-72 \times 10^{-16}$ m$^2$ and tungstates $MWO_4$ ($M$ = Zn, Ca, Sr, and Ba) having $A = 73-82 \times 10^{-16}$ m$^2$. The relatively higher dispersion of $PbWO_4$ can be traced to the presence of $Pb^{2+}$.

In an alternative form of Eq. (1) [10]:

$$n^2 - 1 = E_d E_o / (E_o^2 - (\hbar\omega)^2) \quad (4)$$

where in a single oscillator model: $\hbar\omega$ is the photon energy, $E_o$ the average single oscillator (Sellmeier) energy gap in eV and $E_d$ the average oscillator strength in eV. The parameters $E_o$ and $E_d$ were analyzed for more than 100 compounds [10] and resulted in a scheme that worked well for simple single-bond halides and oxides as well as a number of more complex multi-bond oxides containing 2 cations of differing coordination.

In this scheme, $A = 1/E_oE_d$ and $E_d$ is related empirically by Wemple and Domenico [10] to physical parameters by the expression:

$$E_d = \beta N_c Z_a N_e \quad (5)$$

where $N_c$ is the cation coordination number, $Z_a$ the formal valence of the anion, taking on the value of 2 for oxides, $N_e$ the effective number of valence electrons/anion, 8 for oxides, $\beta = 0.26$ eV for ionic compounds and $\beta = 0.37$ eV for covalent compounds. Table 6 compares $E_d$ observed with $E_d$ calculated using Eq. (5). Although Wemple and Domenico [10] used the coordination number of the nearest-neighbor cation for $N_c$, we find better agreement using the mean cation coordination number $\langle N_c \rangle$. Using the nearest-neighbor cation approach [10] it was necessary to define a new value of $\beta = 0.37$ eV to get agreement with the scheelite compounds $MWO_4$ and $MMoO_4$ but using the mean cation CN of 6, we see satisfactory agreement without resorting to a second value of $\beta$. Furthermore, we obtain reasonable agreement between the observed and calculated values of $E_d$ for $ZrW_2O_8$. The unusually high dispersion is therefore related more to $E_o$ and $N_c$ where lower values of the energy gap, $E_o$ and $N_c$ result in higher dispersions [28].

## 5. Summary

Optical dispersion studies of of $ZrW_2O_8$ allowed the determination of the refractive index, $n_D = 1.8794$, and a total electronic polarizability, $\alpha_{total} = 20.087$ Å$^3$, that is significantly larger than the calculated total polarizability $\alpha_T$ of 17.63 Å$^3$ ($\Delta$ = +12.4%). This large difference relative to that of other tungstates and $Tb(Gd)_2Mo_3O_{12}$ is likely caused by (1) the large Zr–O–W angles (163°) and (2) the presence of terminal O4 and "quasi-terminal" O3 with (a) their large oxygen displacement values, $B$(O), and (b) probable large hybridization of W 5*d*-$O_{(terminal)}$ 2*p* and Zr *nd*–O 2*p* orbitals. The unusually high dispersion of $ZrW_2O_8$ is related to low values of the energy gap, $E_o$, and lower cation coordination number $N_c$, than in other Zr- and W-containing compounds.

## Acknowledgments

We gratefully acknowledge G. Kowach for growth of the $ZrW_2O_8$ crystals, A.W. Sleight for critical reviews of the manuscript and H. Spetzler for encouragement and support at CIRES/CU.

## References

[1] J.S.O. Evans, T.A. Mary, T. Vogt, M.A. Subramanian, A.W. Sleight, Chem. Mater. 8 (1996) 2809–2823.
[2] J.L. Pochou, F. Pichoir, Rech. Aerosp. 3 (1984) 13–38.
[3] O. Medenbach, R.D. Shannon, J. Opt. Soc. Am. B14 (1997) 3299–3318.

[4] X. Gonze, J.-M. Beuken, R. Caracas, F. Detraux, M. Fuchs, G.-M. Rignanese, L. Sindic, M. Verstraete, G. Zerah, F. Jollet, M. Torrent, A. Roy, M. Mikami, Ph. Ghosez, J.-Y. Raty, D.C. Allan, Comput. Mater. Sci. 25 (2002) 478–492.
[5] M. Teter, Phys. Rev. B 48 (1993) 5031–5041.
[6] X. Gonze, C. Lee, Phys. Rev. B 55 (1997) 10355–10368.
[7] S. Sumithra, U.V. Waghmare, A.M. Umarji, Phys. Rev. B 76 (2007) 24307–24312.
[8] L. Ouyang, Y-N. Xu, W.Y. Ching, Phys. Rev. B 65 (2002) 113110–113114.
[9] Z.H. Levine, D.C. Allan, Phys. Rev. Lett. 63 (1989) 1719–1722.
[10] S.H. Wemple, M. DiDomenico, Phys. Rev. B 3 (1971) 1338–1351.
[11] R.D. Shannon, R.X. Fischer, Phys. Rev. B 73 (2006) 235111–235128.
[12] J.D. Jorgensen, Z. Hu, S. Teslic, D.N. Argriou, S. Short, J.S.O. Evans, A.W. Sleight, Phys. Rev. B 59 (1999) 215–225.
[13] R.M. Hazen, L.W. Finger, J.W.E. Mariathasan, J. Phys. Chem. Sol. 46 (1985) 253–263.
[14] R.D. Burbank, Acta Cryst. 18 (1965) 88–97.
[15] M. Auray, M. Quarton, M. Leblanc, Acta Cryst. C51 (1995) 2210–2213.
[16] A. Mary, J.S.O. Evans, T. Vogt, A.W. Sleight, Science 272 (1996) 90–92.
[17] Ph. Ghosez, J.P. Michenaud, W. Gonze, Phys. Rev. B 58 (1998) 6224–6239.
[18] A. Filippetti, N.A. Spaldin, Phys. Rev. B 68 (2003) 45111–45120.
[19] S. Massidda, M. Posternak, A. Baldereschi, R. Resta, Phys. Rev. Lett. 82 (1999) 430–433.
[20] S.Y. Savrosav, G. Kotliar, Phys. Rev. Lett. 90 (2003) 56401–56405.
[21] R.D. Shannnon, J. Appl. Phys. 73 (1993) 348–366.
[22] R.E. Cohen, H. Krakauer, Phys. Rev. B 42 (1990) 6416–6422.
[23] F. Detraux, Ph. Ghosez, X. Gonze, Phys. Rev. B 56 (1997) 983–985.
[24] X. Zhao, D. Vanderbilt, Phys. Rev. B 65 (2002) 75105–75110.
[25] G.-M. Rignanese, X. Gonze, G. Jun, K. Cho, A. Pasquarello, Phys. Rev. B 69 (2004) 184301–184310.
[26] X. Gonze, D.C. Allan, M.P. Teter, Phys. Rev. Lett. 68 (1992) 3603–3606.
[27] C. Lee, X. Gonze, Phys. Rev. Lett. 72 (1994) 1686–1689.
[28] R.D. Shannon, R.C. Shannon, O. Medenbach, R.X. Fischer, J. Phys. Chem. Ref. Data 31 (2002) 931–970.